Astron. Astrophys. 357, 1056–1062 (2000)

ASTRONOMY AND ASTROPHYSICS

Evolution of magnetic field twist in an emerging flux region

Tongjiang Wang[1,2] **and V.I. Abramenko**[1,2,3]

[1] Beijing Astronomical Observatory, Datun Rd. #20A, Chaoyang District, Beijing, 100012, P.R. China (wtj@sun10.bao.ac.cn)
[2] National Astronomical Observatories, Chinese Academy of Sciences, Beijing, 100012, P.R. China
[3] Crimean Astrophysical Observatory, 334413, Nauchny, Crimea, Ukraine

Received 5 November 1999 / Accepted 28 March 2000

Abstract. The observations of vector magnetic field for the emerging active region NOAA 7321 are analyzed. The measurements were performed with SMFT of Huairou Solar Observing Station. The aim is to study the variations of the total flux, total electric current and α parameter (as a measure of the field twist) throughout the flux emergence. We show that: (1) the total positive (negative) electric current grew simultaneously and linearly with the increase of the total positive (negative) flux; (2) the linear extrapolation to the zero flux gives non-vanishing total current which can be regarded as an indirect support for the idea of pre-existing twist of the emerging flux tube; (3) the change in α parameter during three days of the observation was rather small. This fact suggests that α remains the same throughout the flux emergence, and may further explain the good agreement between Longcope et al.'s (1998) simulation of deep thin flux tubes and observations.

Key words: Sun: evolution – Sun: magnetic fields – Sun: photosphere

1. Introduction

Many observational studies have revealed that the solar magnetic field is twisted. This is manifested in various kinds of observations, such as the morphology of H_α structures (Hale 1927; Richardson 1941), the morphology of filaments (Martin et al. 1994), the morphology of coronal loops (Rust & Kumar 1996), and the signs of current helicity derived from vector magnetograms (Seehafer 1990; Pevtsov et al. 1995; Abramenko et al. 1996; Bao & Zhang 1998). All these observations demonstrate a hemispheric preference of the sense of the twist, i.e. the left-handedness in the northern hemisphere and the right-handedness in the southern hemisphere.

It is most likely that the sense of the twist is associated with the solar dynamo and physical conditions of the convection zone (Longcope & Klapper 1997; Longcope et al. 1998). Two mechanisms have been proposed to explain the formation of the twist, i.e., vortical motions of the magnetic plasma (Hofmann & Kalman 1991; Schmieder et al. 1994), and emergence of sub-surface twisted flux (Kurokawa 1987; Tanaka 1991; Wang et al. 1994; Leka et al. 1996).

Many recent investigations of the emerging flux regions have showed that magnetic flux may be already twisted below the photosphere. In the earlier studies, the emergence of twisted sub-surface structures was inferred from the temporal evolution of H_α morphology (Kurokawa 1987; Tanaka 1991). Now high resolution measurement of the photospheric magnetic field enables us to approach this problem quantitatively. Based on the evolution of the magnetic flux and electric current over 6 days, Wang et al. (1994) disclosed that a current system grew rapidly with the emergence of a magnetic loop. In the study of several bipoles that were well-observed within 12 hours since the first detection at white-light, Leka et al. (1996) showed the emerging flux and the electric current were roughly proportional in the growth. They also analyzed the morphology and proper motion of these new bipoles, and concluded that the flux bundles were twisted before their appearance.

In this paper, by using vector magnetograms observed in AR7321, which was a region with a typical EFR, we hope to check the relationship between the emerging flux and electric current, and to study the evolution of the magnetic field twist which can be characterized by the coefficient of the force-free field, α, ($\nabla \times \mathbf{B} = \alpha \mathbf{B}$). These studies may provide new important constrains on theoretical models of flux emergence.

2. Observations

2.1. Instruments and the reliability

The line-of-sight and transverse magnetograms in the photosphere used for this study were obtained with the Solar Magnetic Field Telescope (SMFT) at the Huairou Solar Observing Station (HSOS) (Ai & Hu 1986). This vector magnetograph has a tunable birefringent filter, which can tune its passband working either at the photospheric line FeI λ5324.19 Å, or at the chromospheric line H_β. For the photospheric observations, the passband is tuned at FeI - 0.075 Å to measure longitudinal components of solar magnetic fields, and at the line center to measure transverse components of the fields for achieving the maximum sensitivity. In the measurement of the magnetic field in solar active regions, the integration of 255 frames and the 4×3 average are usually made so as to increase the signal-to-noise

Send offprint requests to: T. Wang

Table 1. List of magnetograms in active region NOAA 7321 in 1992.

Oct.25		Oct.26		Oct.27	
No.	Time (UT)	No.	Time (UT)	No.	Time (UT)
1.....	02:13	7.....	00:46	13.....	00:47
2.....	03:17	8.....	01:38	14.....	01:44
3.....	03:54	9.....	02:31	15.....	02:17
4.....	04:47	10.....	03:01	16.....	02:54
5.....	05:41	11.....	03:34	17.....	03:23
6.....	06:23	12.....	04:53	18.....	04:13

ratio. The magnetograms after the average yield the spatial resolution of about 2″. The calibration of the observed magnetic field has been well established by Ai, Li & Zhang (1982).

Many factors can affect the quantitative measure of the vector magnetic field. Wang et al. (1996) have discussed in detail the limitation and reliability of the HSOS database. They argued that, for the SMFT, the factors such as Zeeman saturation, Doppler shift, Faraday rotation and the cross talk are insignificant. Except for the sunspot umbra area where the contamination of the stray light is serious, the observed line-of-sight flux density is reliable, and the azimuth of the transverse field is reasonably good when a region is close to the disk center. Therefore, both the morphology and the field evolution can be studied from the HSOS vector magnetograms.

2.2. Data reduction

The active region NOAA 7321 was an emerging flux region (EFR), which was born on October 24, 1992 and disappeared at the western limb on November 2. During this period, its configuration underwent a significant change and flares occurred frequently. For this active region, many studies about the features of magnetic topology and flares have been done (Takakura et al. 1994; Zhang 1995; Wang 1997; Liu et al. 1995, 1998; Wang, Qiu & Zhang 1998; Wang, Wang & Qiu 1999; Wang, Yan & Sakurai 1999; Qiu et al. 1999).

We chose 18 magnetograms within 3 days (listed in Table 1) for our study. The active region was situated at the positions from (E9, S23) to (W20, S23) on the solar disk during this period. As it was very close to the disk center, projection effect on the magnetic data was not significant. So we did not transform the data into the heliospheric plane. On the other hand, this avoids the contamination to the vertical components by the projection correction, because the noise level of transverse field measurements is generally higher than that of longitudinal field measurements by an order of magnitude. Hereafter in this paper we take $B_{//}$ as B_z. The 180° ambiguity of the transverse field measurements was resolved by a multistep method (Wang et al. 1994).

The total magnetic flux for a region of interest (S) is calculated by

$$\Phi = \int_S B_z dS = \sum_{\Omega(2\sigma_{Bz})} B_z dS, \tag{1}$$

where $\Omega(2\sigma_{Bz}) = S(|B_z| > 2\sigma_{Bz})$, i.e., the area with B_z above the $2\sigma_{Bz}$ level in the region S. We estimated σ_{Bz} as the standard deviation of the longitudinal field measurement, while σ_{Bt} as the average value of the transverse field measurement, both for a weak-field area. Errors in the sum for Φ are mainly determined by $\Omega(\sigma_{Bz})$, thus we estimated the errors using

$$\begin{aligned}\Delta\Phi &= \sum_{\Omega(2\sigma_{Bz})} B_z dS - \sum_{\Omega(3\sigma_{Bz})} B_z dS \\ &= \Phi(2\sigma_{Bz}) - \Phi(3\sigma_{Bz}).\end{aligned} \tag{2}$$

Similarly, the total current is calculated by

$$I = \int_S J_z dS = \sum_{\Omega(2\sigma_{Bt})} J_z dS, \tag{3}$$

where

$$J_z = \frac{1}{\mu_0}\left(\frac{\partial B_y}{\partial x} - \frac{\partial B_x}{\partial y}\right), \tag{4}$$

and

$$\Omega(2\sigma_{Bt}) = S(|B_t| > 2\sigma_{Bt}). \tag{5}$$

J_z is deduced with the differencing method for the filtered transverse field measurement with a relative cutoff frequency, 20 (Wang, Qiu & Zhang 1998; Wang, Wang & Qiu 1999). The error of I is given by

$$\Delta I = \sum_{\Omega(2\sigma_{Bt})} J_z dS - \sum_{\Omega(3\sigma_{Bt})} J_z dS = I(2\sigma_{Bt}) - I(3\sigma_{Bt}). \tag{6}$$

A convenient way to characterize the twist in magnetic flux is to use the force-free field parameter α which has the physical meaning of current helicity (Pevtsov et al. 1994, 1995). From the measured field the distribution of α can be obtained ($\alpha = J_z/B_z$). The global estimate of twist can be estimated by averaging α over the region of interest S where $B_t > 2\sigma_{Bt}$ and $B_z > 2\sigma_{Bz}$ are satisfied.

$$\alpha_{avg} = \frac{1}{N}\sum_S \alpha, \tag{7}$$

An improved calculation method is to average α weighted by the element flux $d\phi$, which gives a more clear physical implication. If each field line is given a single value of α, then the average of α for a bundle of field lines in a region should be,

$$\alpha_{avw} = \frac{\int_s \alpha d\phi}{\int_s d\phi} = \frac{\sum \alpha |B_z| dS}{\sum |B_z| dS}. \tag{8}$$

The α_{avw} describes the twist which is representative of most field lines.

Alternatively, the twist of an entire AR, supposedly a linear force-free field, can be described by a single constant α which is computed from the observed longitudinal field boundary and best fits the transverse components. Two methods can be used to achieve an optimal fit. The first method minimizes the difference

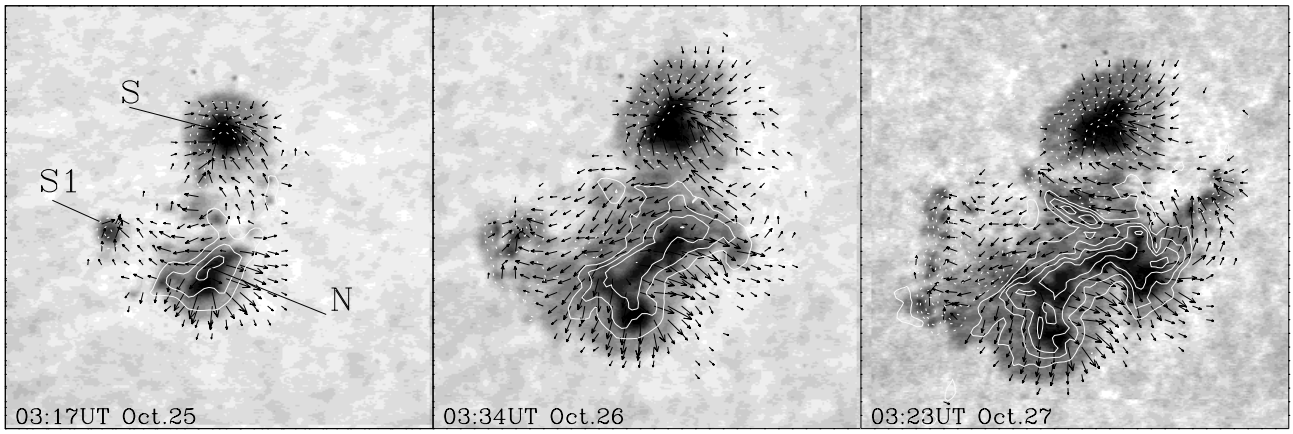

Fig. 1. The photospheric vector magnetograms (contours) superposed on the white light images showing the spots. The white contours in all figures demonstrate the intensity of the longitudinal field (levels = ±500, 1500, 2500, and 3500 Gauss); solid lines show the positive field and dashed lines show the negative field. The short arrows indicate the transverse field with the intensity above $2\sigma_{Bt}$ noise level. The field of view (FOV) is $157'' \times 157''$.

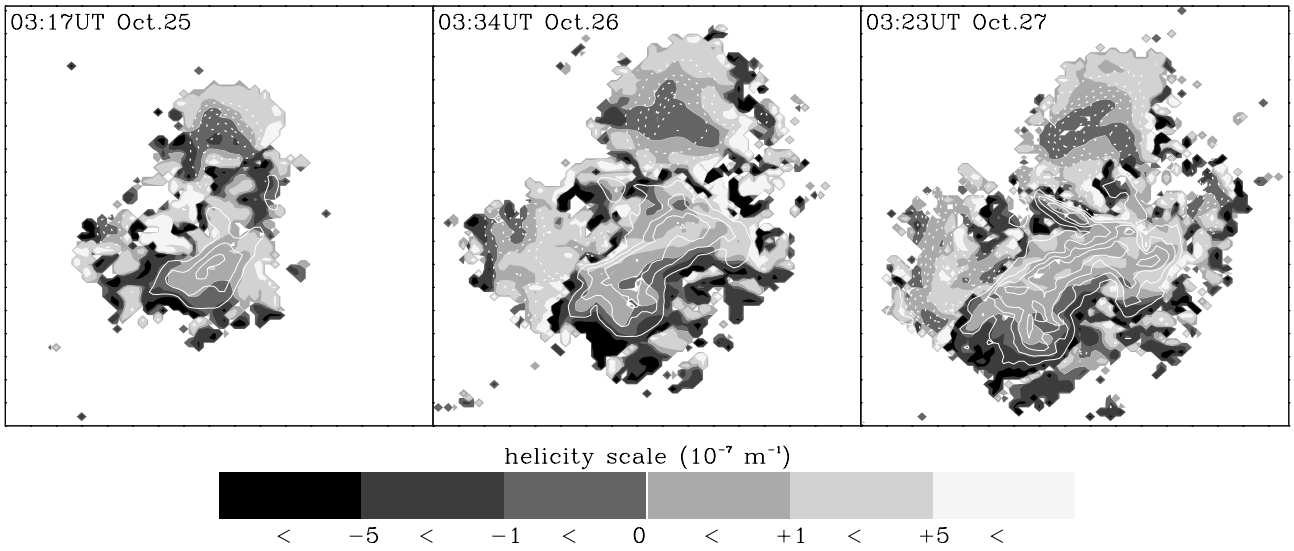

Fig. 2. Maps of α density (gray-scale) with the photospheric magnetograms superposed on. The white solid (dashed) contours show positive (negative) fields with the same levels as in Fig. 1. The α scale (units of $10^{-7}\mathrm{m}^{-1}$) is shown below. The grey maps only show α distribution in such areas where $B_t > 2\sigma_{Bt}$ and $B_z > 2\sigma_{Bz}$. The field of view is the same as in Fig. 1.

between the x and y components of the computed and observed fields (Pevtsov et al. 1995),

$$\alpha_{dif} = \alpha(R_{min}),$$
$$R = \frac{1}{N}\sum[(B_{xo} - B_{xc})^2 + (B_{yo} - B_{yc})^2], \quad (9)$$

where B_{xo}, B_{yo} are the x and y components of the observed field, and B_{xc}, B_{yc} are those of the computed field. The second method minimizes the angles between the transverse components of the computed and observed fields (Wang, Yan & Sakurai 1999),

$$\alpha_{ang} = \alpha(R_{min}), \quad R = cos^{-1}\left(\frac{1}{N}\sum\frac{|\mathbf{B}_{to}\cdot\mathbf{B}_{tc}|}{B_{to}B_{tc}}\right), \quad (10)$$

where $\mathbf{B}_{to}$, $\mathbf{B}_{tc}$ are the transverse components of the observed and computed fields, respectively. We adopted the optimum technique to determine the value of α_{best} which satisfies the condition $(R^n_{min} - R^{n+1}_{min})/R^n_{min} < 1\%$. An advantage in the α_{ang} method is that the determination of its value does not depend on the 180°-ambiguity resolution of the observed transverse field.

3. Results

For all 18 magnetograms (see Table 1) we calculated the total flux and the error bars using Eqs. (1) and (2), respectively; and calculated the total positive and negative currents and the error bars using Eqs. (3) and (6), respectively. Along with this we estimated the value of α in four ways, i.e. using Eqs. (7), (8), (9) and (10). In the latter two cases we calculated the linear force-free field by the Fourier Transform Method (Alissandrakis 1981). Such algorithms were performed both for the entire active region and for the three main spots separately.

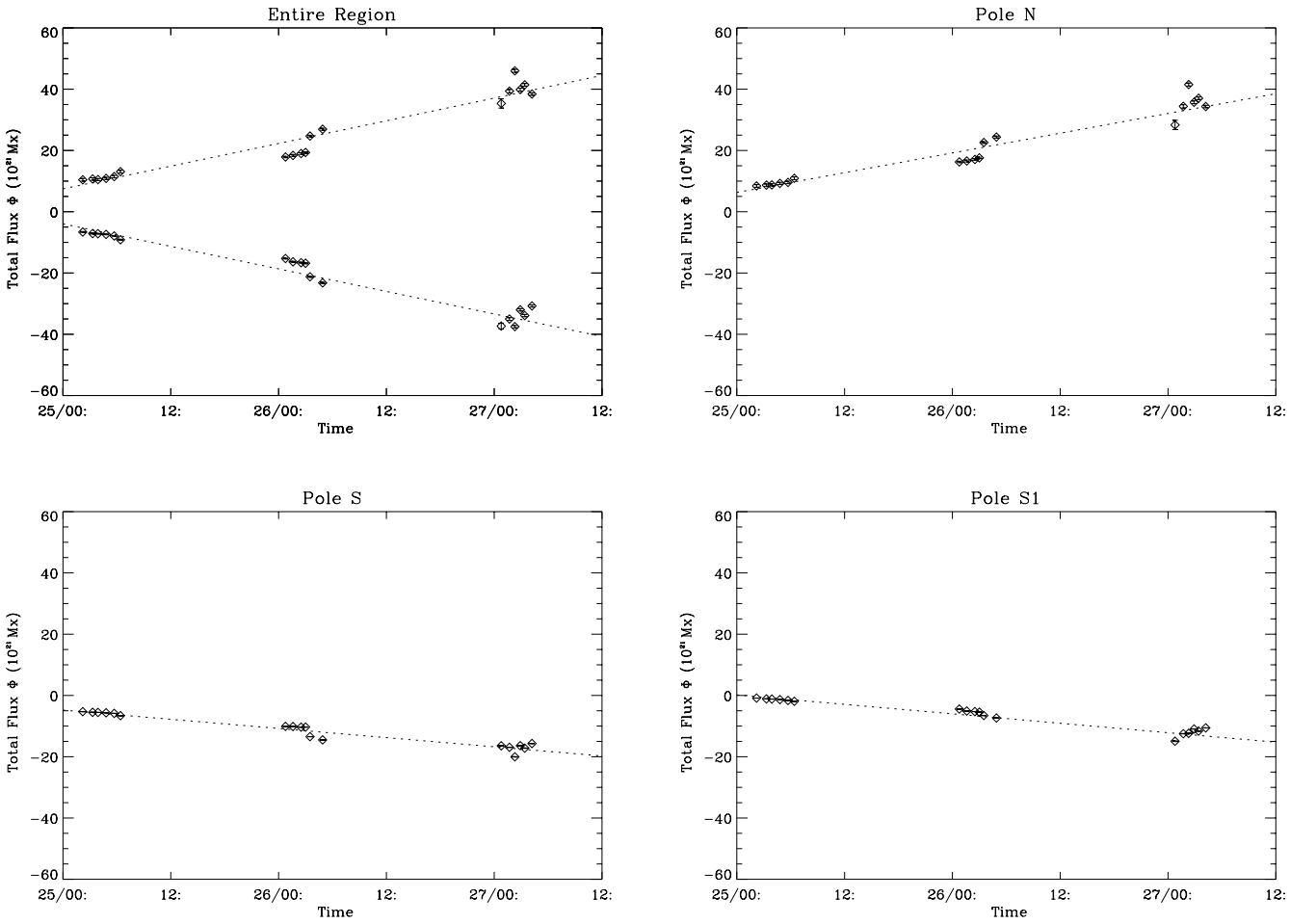

Fig. 3. Time variations of the total flux (Φ) for the entire region and for the main poles (N, S and S1). The bars for Φ do not exceed the size of symbols. The dashed lines represent a least-square linear fit.

Fig. 1 shows the daily vector magnetograms of the active region. The emergence of the magnetic flux is well pronounced. Three main poles can be revealed: N, S and S1. The corresponding daily maps of α density ($\alpha = J_z/B_z$) are presented in Fig. 2. In Figs. 3 and 4 the time variations of the total fluxes Φ and total currents I are shown. The monotonous growth of the total flux both in the entire AR and in the N, S and S1 poles is obvious. The same is valid also for the total currents, except for the total positive currents in S and S1: they are weak and practically constant. The growth rates of the flux and current (estimated from the least-square linear fit in Figs. 3 and 4) are presented in Table 2. One can see that the growth rate of the total positive flux (current) is very close to that of total negative flux (current) for the entire AR. Such a situation can be physically interpreted by the solenoidal nature of $\mathbf{B}$ and $\mathbf{J}$ vectors, and this confirms the reliability of our field measurement and current calculations.

The plot of the total current versus the total flux is shown in Fig. 5. It is shown that for the entire AR there are two linear relationships: for the positive branch (with the coefficient $dI^+/d\Phi^+ = 6.0 \times 10^{-8} m^{-1}$) and for the negative branch (with the coefficient $dI^-/d\Phi^- = 6.3 \times 10^{-8} m^{-1}$). Moreover, in both cases, the least-square linear fit does not cross the zero.

Table 2. Growth rates of the total flux and the total current.

Region	$\frac{d\phi}{dt}^+$ (10^{21}Mx/hr)	$\frac{d\phi}{dt}^-$ (10^{21}Mx/hr)	$\frac{dI}{dt}^+$ (10^{12}A/hr)	$\frac{dI}{dt}^-$ (10^{12}A/hr)
Whole	0.62	-0.61	0.32	-0.32
N	0.54	—	0.26	-0.12
S	—	-0.25	0.007	-0.086
S1	—	-0.26	0.013	-0.068

When $\Phi^+ \to 0$, $I^+ \to 3 \times 10^{12}$A, and for $\Phi^- \to 0$ we have $I^- \to -5 \times 10^{12}$A. In each of the poles studied, there are both positive and negative currents, but the positive (negative) current dominates in the N pole (S, S1 poles). This results in the overall positive (right-handed) twist in the entire AR, which can be estimated from $dI/d\Phi$ by the least-square linear fit in Fig. 5. The results of this estimation are shown in Columns (2) and (4) in Table 3. Columns (3) and (5) represent the coefficient of the Spearman rank correlation (Press et al. 1994). One can see that the correlations are high enough.

The results of direct calculations of α by Eqs. (7), (8), (9) and (10) are given in Fig. 6 and Table 4. The comparison of α calculated by different approaches allows us to conclude that the

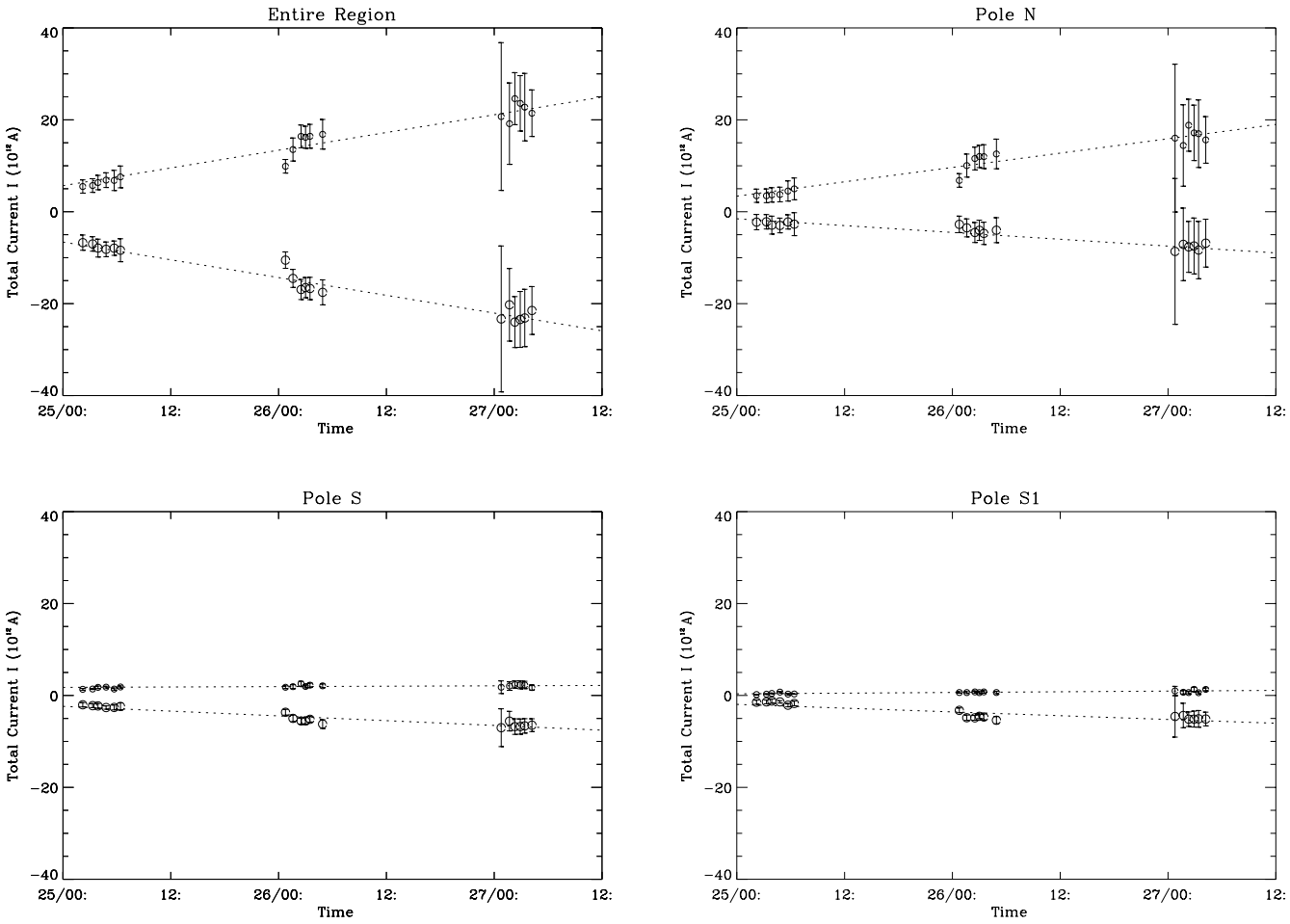

Fig. 4. Time variations of the total positive and negative currents (I) for the entire region and for the main poles (N, S and S1). The dashed lines represent a least-square linear fit.

Table 3. Slope coefficients of the least-square linear fit for the total flux and the total current, and coefficients of the Spearman rank correlation.

Region	$\frac{dI^+}{d\Phi^+}$ (10^{-8}m^{-1})	ρ_+	$\frac{dI^-}{d\Phi^-}$ (10^{-8}m^{-1})	ρ_-
Whole	6.0	0.98	6.3	0.97
N	5.3	0.98	—	—
S	—	—	4.2	0.95
S1	—	—	8.3	0.75

Table 4. Four estimates of α parameter averaged over 3 days. All forms have the same unit of 10^{-8}m^{-1}.

Region	α_{avg}	α_{avw}	α_{ang}	α_{dif}
Whole	5.5±2.2	3.9±1.3	2.7±1.2	3.2±1.5
N	-4.6±2.5	3.4±1.3	1.2±0.7	2.4±1.3
S	14±5	3.1±1.4	1.0±0.9	0.7±0.9
S1	26±13	10.±4.4	4.4±1.9	5.0±1.2

$|\alpha|$ is systematically larger when estimated as α_{avg} (Column (2) in Table 4). Moreover, in the pole N the α_{avg} is negative that disagrees with other forms of α estimation in this pole (α_{avw}, α_{ang} and α_{dif}). This may be caused by the presence of large negative α in places of weak field. These places should not weigh a lot in the total twist. So this case (pole N) shows that the α_{avg} method has some intrinsic disadvantage as compared with the α_{avw} method. In addition, α_{avw} shows the better coincidence in values with α_{ang} and α_{dif} as well as the estimate of α from $dI/d\Phi$ (see Tables 3 and 4). This also suggests that the α_{avw} method seems more reasonable than the α_{avg} method to measure the twist of the flux.

So, except α_{avg}, all other estimated α are in a good agreement to show that the changes in α from day to day were rather small. This result indicates that the twist, or, the magnetic complexity, changes very slowly during the flux emergence.

4. Conclusions and discussions

From the analysis of 18 vector magnetograms of an emerging active region NOAA 7321 we have obtained the following results:

1. The total flux and total current grew synchronously, following a linear relationship, but such a linear relationship between the growth rate of the flux and that of the current is different for positive and negative regions.

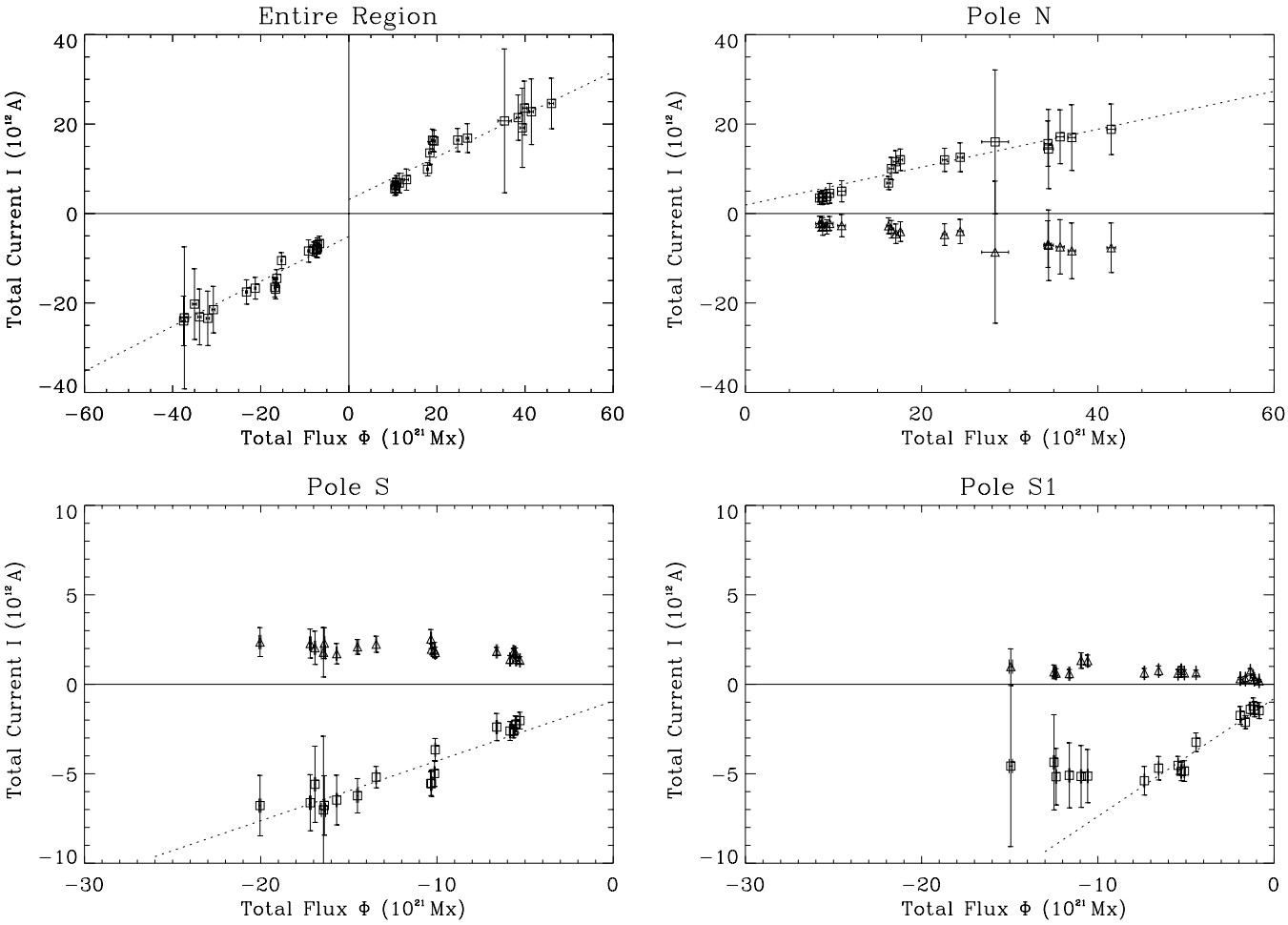

Fig. 5. The total current (I) versus the total flux (Φ) for the entire region and for the main poles (N, S and S1). *Squares* refer to positive α; *Triangles* refer to negative α. The dashed lines represent a least-square linear fit.

2. The linear extrapolation of the electric current, $I^{\pm}$, to the zero magnetic flux, $\Phi^{\pm}$, did not vanish, but produces a value of about 3×10^{12}A and -5×10^{12}A for positive and negative regions respectively.
3. The change in α (as a measure of the total twist of the AR) was rather small; during 3 days of flux emergence, α remained at about $6\times10^{-8}\mathrm{m}^{-1}$.

Our first result coincides in general with that of Leka et al. (1996). The second result is more surprinsing. One possible explanation is that the photospheric magnetic field is not force-free (Metcalf et al. 1995; Abramenko & Yurchishin 1997), so the current $\mathbf{J}$ may be not parallel to $\mathbf{B}$. Therefore, at the very beginning of the tube emergence, when the field $\mathbf{B}$ in the tube is almost horizontal, the $\mathbf{J}$ may have the vertical component. Besides, some pre-existing total current due to small-scale magnetic field in quiet regions (Abramenko et al. 1992) should be present in the area where the flux tube emerges. In any case, the non-vanishing total current at the vanishing total flux does not contradict the idea on the sub-photospheric pre-existing twist of the emerging flux tube.

According to our third result, the measured twist seems to keep constant during the emergence. This means that the topology complexity of the emerging flux system is an invariable. Moreover, this result is very important for the validity of Longcope et al. (1998) simulations of the twist evolution in the thin flux tube model. This model is restricted by sub-photospheric thin flux tubes in the depth not less than 30 Mm below the photosphere, since above this depth, the radius of the flux tube will expand rapidly so that the equations to describe the thin tube will no longer be valid. Nevertheless, such simulation shows a good agreement with the observations in both mean value and statistical dispersion of α for 203 ARs (Longcope et al. 1998). The underlying cause for this agreement seems to be the small change of α (twist) throughout the emergence.

Acknowledgements. We thank Prof. Wang J.X. and Dr. Wang H.N. for helpful discussions, the referee, Dr. J.L. Ballester, for helpful comments, and Dr. Qiu J. for improving the manuscript in language. This work is supported by the National Natural Science Foundation of China (NSFC), under grants 19791090 and 49990450.

References

Abramenko V.I., Gopasyuk S.I., Ogir M.B., 1992, Bull. Crimean Astrophys. Obs. 84, 117

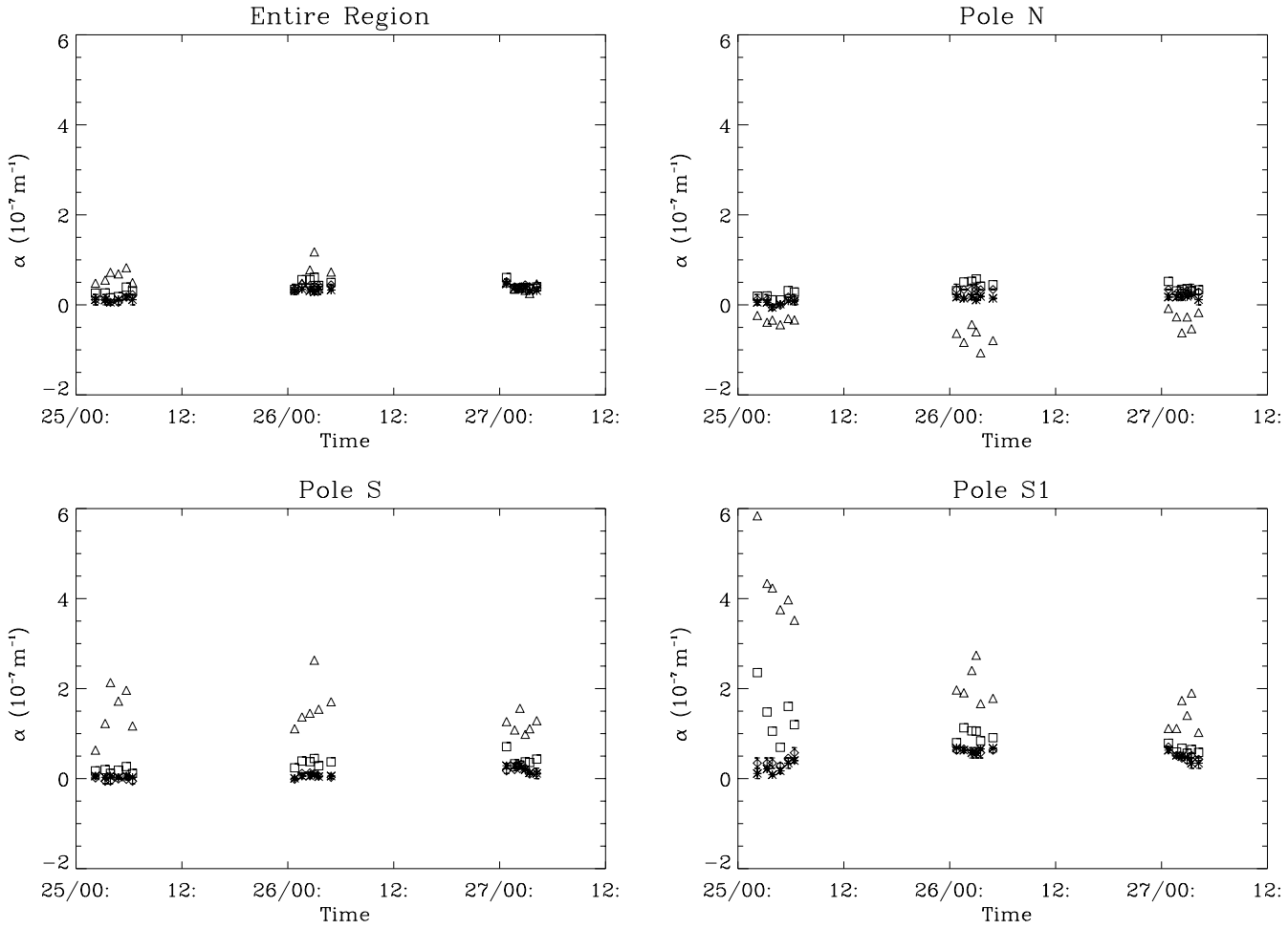

Fig. 6. Time variations of four forms of the parameter α characterizing the twist of the flux for the entire AR and for the main poles (N, S and S1). *Triangles*: α_{avg}, the average of α. *Squares*: α_{avw}, the average of α weighted by the flux element $d\phi$. *Diamonds*: α_{dif}, the best-fit α of a constant force-free field which minimizes the difference between the x and y components of the computed and observed fields. *Asterisks*: α_{ang}, the best-fit α which minimizes the angles between the transverse components of the computed and observed fields. In the former two cases, α is averaged only over pixels with $B_t > 2\sigma_{Bt}$ and $B_z > 2\sigma_{Bz}$, while in the latter two cases, the regions of average satisfy the condition $B_t > 2\sigma_{Bt}$.

Abramenko V.I., Wang T., Yurchishin V.B., 1996, Solar Phys. 168, 75

Abramenko V.I. Yurchishin V.B., 1997, Kinematics Phys. Celest. Bodies 12(6), 3

Ai G., Hu Y., 1986, Publ. Beijing Astron. Obs. 8, 1

Ai G., Li W., Zhang H., 1982, Chin. A&A 6, 129

Alissandrakis C.E., 1981, A&A 100, 197

Bao S., Zhang H., 1998, ApJ 496, L93

Hale G.E., 1927, Nat 119, 708

Hofmann A., Kalman B., 1991, A&A 241, 203

Kurokawa H., 1987, Solar Phys. 113, 259

Leka K.D., Canfield R.C., McClymont A.N., Van Driel-Gesztelyi L., 1996, ApJ 462, 547

Liu Y., Srivastava N., Prasad D., Li W., Ai G., 1995, Solar Phys. 158, 249

Liu Y., Akioka M., Yan Y., Ai G., 1998, Solar Phys. 177, 395

Longcope D.W., Klapper I., 1997, ApJ 488, 443

Longcope D.W., Fisher G.H., Pevtsov A.A., 1998, ApJ 507, 417

Martin S.F., Billamoria R., Tracadas P.W., 1994, In: Rutten R.J., Schrijver C.J. (eds.) Solar Surface Magnetism. Kluwer, Dordrecht, p. 303

Metcalf T.R., Jiao L., McClymont A.N., Canfield R.C., Uitenbroek H., 1995, ApJ 439, 474

Pevtsov A.A., Canfield R.C., Metcalf T.R., 1994, ApJ 425, L117

Pevtsov A.A., Canfield R.C., Metcalf T.R., 1995, ApJ 440, L109

Press W.H., Teukolsky S.A., Vetterling W.T., Flannery B.P., 1994, In: Numerical Recipes in Fortran. Second Edition, Cambridge University Press, p. 634

Qiu J., Xu A., Wang T., 1999, Chin. Space Science 19, 7

Richardson R.S., 1941, ApJ 93, 24

Rust D.M., Kumar A., 1996, ApJ 464, L199

Schmieder B., Hagyard M.J., Ai G., et al., 1994, Solar Phys. 150, 199

Seehafer N., 1990, Solar Phys. 125, 219

Takakura T., Nishio M., Nakajima H., et al., 1994, PASJ 46, 653

Tanaka K., 1991, Solar Phys. 136, 133

Wang H.N., 1997, Solar Phys. 174, 265

Wang H.N., Yan Y., Sakurai T., 1999, Solar Phys., submitted

Wang J., Shi Z., Wang H., Lü Y., 1996, ApJ 456, 861

Wang T., Xu A., Zhang H., 1994, Solar Phys. 155, 99

Wang T., Qiu J., Zhang H., 1998 A&A 336, 359

Wang T., Wang H.N., Qiu J., 1999, A&A 342, 854

Zhang H., 1995, A&A 304, 541